ADVANCES IN MATERIALS SCIENCE, Vol. 23, No. 2 (76), June 2023

DOI: 10.2478/adms-2023-0009

Anouar Saidi[1*], Ahmed M.H Yahya[1,2], Ahmed E. Abouelregal[1,3], Husam E. Dargail[1,2] Ibrahim-Elkhalil Ahmed[1,2], Elsiddeg Ali[4], F. A. Mohammed[1,5]

[1]*Department of Mathematics, College of Science and Arts of Gurayyat, Jouf University, Gurayyat, Kingdom of Saudi Arabia*
[2]*Department of Mathematics, Faculty of Science and Technology, Shendi University, Shendi, Sudan*
[3]*Department of Mathematics, Faculty of Science, Mansoura University, Mansoura, 35516, Egypt*
[4]*Department of Mathematics, Taif University Faculty of Science, Kingdom of Saudi Arabia*
[5]*Department of Mathematics, Faculty of Science, South Valley University, Qena, Egypt*

** saidi.anouar@yahoo.fr*

GENERALIZED THERMOELASTIC HEAT CONDUCTION MODEL INVOLVING THREE DIFFERENT FRACTIONAL OPERATORS

ABSTRACT

The purpose of this paper is to introduce a new time-fractional heat conduction model with three-phase-lags and three distinct fractional-order derivatives. We investigate the introduced model in the situation of an isotropic and homogeneous solid sphere. The exterior of the sphere is exposed to a thermal shock and a decaying heat generation rate. We recuperate some earlier thermoelasticity models as particular cases from the proposed model. Moreover, the effects of different fractional thermoelastic models and the effect of instant time on the physical variables of the medium are studied. We obtain the numerical solutions for the various physical fields using a numerical Laplace inversion technique. We represent the obtained results graphically and discuss them. Physical views presented in this article may be useful for the design of new materials, bio-heat transfer mechanisms between tissues and other scientific domains.

Keywords: *Thermoelasticity; Fractional order; Three-phase-lags; Solid sphere*

INTRODUCTION

The theory of thermoelasticity covers many phenomena. It embraces the theory of heat conduction, strains and stresses owing to the flow of heat. It is mainly interested in the mutual influence between the distribution of the strains and the thermal state in an elastic medium .

Likewise, it helps us to determine the thermal stresses produced by the temperature field and to calculate the temperature distribution due to the action of internal forces.

Historically, Neumann [1] and Duhamel [2] formulated the theory of uncoupled thermoelasticity. A significant shortcoming of this theory is that it neglects the effect of the deformation on the temperature of an elastic body, which contradicts physics observations. To avoid this contradiction, Biot [3] announced the theory of coupled thermoelasticity by including inertia terms in the equation of motion. However, both theories predict a

propagation for the temperature with an infinite speed, which is in discordance with true physical experiments.

Cattaneo [4, 5], Vernotte [6], Lord and Shulman [7], Green and Lindsay [8] and others modified the classical law of heat conduction (Fourier's law) by including the time derivative of the heat flux vector and thus formulated the new theory of generalized thermoelasticity for an isotropic medium. This new model, with a single phase-lag, is known as the Lord and Shulman model (LS). By this model, the equation of heat is hyperbolic and therefore removes the contradiction of infinite speeds of propagation. Nevertheless, the (LS) theory did not take into account the microstructural effects that arise in high-rate heat transfer.

Tzou [9-11] proposed the dual-phase lag model (DPL) by introducing two phase-lag parameters to the heat flux and the temperature gradient in the heat conduction law. This famous model is supposed to bring together among the macroscopic and the microscopic approaches, involving numerous models of heat transfer. The (DPL) model has also fascinated many scientists in a varied range of physical and technical domains [12-16]. Unfortunately, this model cannot represent a general form of all the Green and Naghdi models [17-19].

Roy Choudhuri [20 was the first to formulate the three-phase-lag theory (TPL) as a generalization of the (DPL) model by adding a third phase-lag to the thermal displacement gradient. Through this model, one can recuperate the new theories of Green and Naghdi (GN II and GNIII).

Thermoelasticity models have many and varied applications in various scientific fields. In aviation [21-25], the high speed of the aircraft causes aerodynamic heating which firstly leads to high thermal stress and secondly weakens the airframe. In the field of nuclear sciences [26-29], the design and operation of nuclear reactors are affected by the exceptionally high temperatures they generate. Besides, research in the domain of thermoelasticity becomes growingly important concerning the efficacy analysis of rocket engine technology [30], spacecraft technologies, Laser machining [31], the mechanics of steam turbines [32-34] and in ship construction where moderate thermal stresses frequently cause ships to crack.

Leibniz and L'Hospital, in 1695, in their famous correspondence [35], were the first to introduce the concept of fractional calculus but the complete theory was developed from the 19th century by Lacroix [36], Liouville [37, 38], Fourier [39], Riemann [40], Sonin [41], Laurent [42], Grunwald [43], Weyl [44] and others. However, this theory became more interesting in the last decades [45] since it is more precise in the modelling of real scientific phenomena deriving from numerous scientific fields such as control and robotics [46, 47], wave and diffusion propagation [48, 49], electromagnetic waves [50], biomedicine and biology [51], viscoelastic systems [52, 53].

One of the first scientists to use fractional calculus in the mathematical modelling of thermoelasticity theories was Povstenko. He successfully modelled an uncoupled quasi-static theory of thermoelasticity [54] and studied axisymmetric thermal stresses in an elastic medium provided with a hollow cylinder [55]. Youssef [56] gave a fractional thermoelasticity model taking into account the work of Povstenko and the generalized theory of Lord and Shulman. Besides, he established the uniqueness theorem and studied an application to an elastic half-space medium.

The aim of the current paper is to introduce and investigate a new model of generalized thermoelasticity with three-phase delays and three different fractional-order derivatives. We denote this modified model by the generalized fractional three phase-lag model (GFTPL). Recently, Sherief et al. [57] proposed a fractional thermoelasticity model with single phase-lag named fractional Lord and Shulman model (FLS). Xu et al. [58, 59] constructed two fractional thermoelastic models called fractional dual-phase-lag (FDPL) and generalized fractional dual-phase-lag (GFDPL). Ezzat et al. [60] studied a fractional thermoelasticity

theory with three-phase-lags (FTPL) and Abouelregal [61] investigated a new thermoelastic model with higher-order-time-fractional derivatives and three-phase-delays (HFTPL). These models are more general than other thermoelastic models and allow us to recuperate a great number of anterior theories of thermoelasticity.

In the present work, the heat transfer problem of an isotropic solid sphere subjected to a decreasing heat generation rate with time was examined to verify the accuracy of the proposed model. To provide a solution to this problem, a Laplace transform and an accurate numerical algorithm method have been applied to map the inversions of the Laplace transform. Distributions of domain variables such as temperature, displacement, and thermal pressure were calculated. To study the interactions between the parameters of the fractional derivatives and the instantaneous time, graphic representations of the obtained numerical results were presented.

Quintanilla [62] gave conditions on the specific material properties to ensure the exponential stability of the solution of thermoelastic models with three phase-lags. The same author [63] studied the well-posedness of the related problems. Chirita et al [64] studied the thermodynamic compatibility of the same models. By comparing the results of the current model and previous models, the accuracy of the obtained results is shown in accordance with the experimental and physical results. The new model of heat conduction transport has some interesting features that need to be taken into account. We believe that the results of this topic will be an excellent way to understand the behavior of many different models.

GOVERNING EQUATIONS OF THERMOELASTICITY THEORY

Fractional calculus has been used successfully in many scientific fields, such as complex systems [65] and anomalous diffusion [66, 67]. In this section, we will come up with a modified law of thermoelasticity that includes three fractional derivatives with different differential orders.

Green and Naghdi [17-19] elaborated two theories of thermoelasticity for homogeneous and isotropic materials, which are significantly different from the conventional one. The second theory, named the Green and Naghdi III model (GN-III), is obtained by adding a new constitutive variable to the classical Fourier's law. This new variable, named thermal displacement, is usually interpreted as the counterpart in thermal fields of mechanical displacement in mechanical fields. The (GN-III) model includes dissipation of energy and allows damped waves. The heat conduction law [18] for this model is given by

$$\mathbf{q}(x,t) = -K\,\nabla T(x,t) - K^{*}\,\nabla\vartheta(x,t) \tag{1}$$

where $\mathbf{q}$ is the heat flux, K is the thermal conductivity, K^{*} is a positive constant [18], T is the temperature-change above a uniform temperature T_0 of the medium verifying $|T - T_0|/T_0 \ll 1$. We denote $\theta = T - T_0$ the thermodynamic temperature and ϑ the thermal displacement [19] verifying $\frac{\partial\vartheta}{\partial t} = \theta$.

Extending the (GN-III) model given in equation (1), Roy Choudhury [20] constructed a model of heat conduction with three phase-lag (TPL). The author added a new phase-delay of the thermal displacement gradient $\nabla\vartheta$ additionally to the classical phase-lags $\tau_{\mathbf{q}}$ and τ_{θ} of heat flux and temperature gradient. The heat conduction law of the (TPL) model takes the form

$$\mathbf{q}\big(x,t+\tau_{\mathbf{q}}\big) = -K\,\nabla\theta(x,t+\tau_{\theta}) - K^{*}\,\nabla\vartheta(x,t+\tau_{\vartheta}) \tag{2}$$

In this last equation, we notice that the temperature gradient and the thermal displacement gradient obtained at a fixed position x, at instances $t+\tau_{\theta}$ and $t+\tau_{\vartheta}$, ensue in heat flux

flowing at an instance of time $t+\tau_q$. This gives a physical explanation of the new phase-lag τ_ϑ.

Using an order one Taylor expansion, Eq. (2) yields

$$\left(1+\tau_{\mathbf{q}}\,\frac{\partial}{\partial t}\right)\mathbf{q}=-K\left(1+\tau_\theta\,\frac{\partial}{\partial t}\right)\nabla\theta-K^*\left(1+\tau_\vartheta\,\frac{\partial}{\partial t}\right)\nabla\vartheta \tag{3}$$

The concept of classical calculus has been generalized by introducing the concept of non-integer calculus (historically named fractional order calculus) in several ways, which led to many definitions [45], [68-70]). In the present work, Caputo [68] definition of the fractional derivative of order α $(0<\alpha\leq 1)$ will be applied to any suitable function $f(t)$. It is defined by the relation:

$$\frac{\partial^\alpha}{\partial t^\alpha}\,f(t)=(I^{1-\alpha}f')(t) \tag{4}$$

where I^α is the Riemann–Liouville integral operator of order α defined by

$$I^\alpha f(t)=\int_0^t\frac{(t-\tau)^{\alpha-1}}{\Gamma(\alpha)}f(\tau)\mathrm{d}\tau \tag{5}$$

We replace, in Eq (3), the first order derivative $\frac{\partial}{\partial t}$ by fractional derivatives defined in Eq. (4), and the phase-lags $\tau_{\mathbf{q}}$, τ_θ and τ_ϑ by $\tau_{\mathbf{q}}^\alpha$, τ_θ^β and τ_ϑ^δ, providing that the continuous functions $\mathbf{q}$, θ and ϑ have fractional derivatives of order (α,β and δ respectively) where $0<\alpha,\beta,\delta\leq 1$. Thus, our new fractional model is given by

$$\left(1+\tau_{\mathbf{q}}^\alpha\,\frac{\partial^\alpha}{\partial t^\alpha}\right)\mathbf{q}=-K\left(1+\tau_\theta^\beta\,\frac{\partial^\beta}{\partial t^\beta}\right)\nabla\theta-K^*\left(1+\tau_\vartheta^\delta\,\frac{\partial^\delta}{\partial t^\delta}\right)\nabla\vartheta \tag{6}$$

Since the parameters of the phase-lags $\tau_{\mathbf{q}}$, τ_θ and τ_ϑ are different from each other, the three fractional order parameters α, β and δ are also different but can be equal in some applications.

The classical energy equation is formulated by

$$-\nabla.\mathbf{q}+\rho Q=\rho C_e\,\frac{\partial\theta}{\partial t}+\gamma T_0\,\frac{\partial}{\partial t}(\nabla.\mathbf{u}) \tag{7}$$

where C_e is the constant specific heat, $\gamma=(3\lambda+2\mu)\alpha_t$ denotes the stress temperature modulus where α_t represents the thermal expansion coefficient, λ, μ are Lamé's constants, ρ is the density of the medium and Q is magnitude of the heat source.

Combining Eq. (6) and Eq. (7), we obtain

$$K\left(1+\tau_\theta^\beta\,\frac{\partial^\beta}{\partial t^\beta}\right)\nabla^2\theta+K^*\left(1+\tau_\vartheta^\delta\,\frac{\partial^\delta}{\partial t^\delta}\right)\nabla^2\vartheta+\left(1+\tau_{\mathbf{q}}^\alpha\,\frac{\partial^\alpha}{\partial t^\alpha}\right)\rho Q=\left(1+\tau_{\mathbf{q}}^\alpha\,\frac{\partial^\alpha}{\partial t^\alpha}\right)\left(\rho C_e\,\frac{\partial\theta}{\partial t}+\gamma T_0\,\frac{\partial}{\partial t}(\nabla.\mathbf{u})\right) \tag{8}$$

Equation (8) describes some previous models of thermoelasticity for different values of the parameters $\tau_{\mathbf{q}}$, τ_θ, τ_ϑ and α, β, δ as follows:

- When $K^*=0$, $\tau_\theta=0$ and $\alpha=1$, we obtain the (LS) model [7].
- Taking $K^*=0$ and $\alpha=\beta=1$, we get the dual-phase-lags theory (DPL) proposed by Tzou [11].
- When $\tau_{\mathbf{q}}=\tau_\theta=\tau_\vartheta=0$, we obtain the (GN III) model [18].
- When $\alpha=\beta=\delta=1$, we recuperate the (TPL) model [20] of thermoelasticity theory with three-phase-lags.
- When $K^*=0$ and $\tau_\theta=0$, we can obtain the fractional thermoelasticity model with single phase-lag (FLS) [57].
- The Fractional thermoelasticity theory with dual-phase-lags (FDPL) formulated by Xu et al. [58] can be obtained when $K^*=0$ and $\alpha=\beta$.

- Fractional thermoelasticity theory with three-phase-lags (FTPL) is obtained when $\alpha = \beta = \delta$. Ezzat et al. [60] introduced this model with the terms $\frac{\tau_{\mathbf{q}}^{\alpha}}{\alpha!}\frac{\partial^{\alpha}}{\partial t^{\alpha}} + \frac{\tau_{\mathbf{q}}^{2\alpha}}{(2\alpha)!}\frac{\partial^{2\alpha}}{\partial t^{2\alpha}}$ instead of $\tau_{\mathbf{q}}^{\alpha}\frac{\partial^{\alpha}}{\partial t^{\alpha}}$.
- The (GFDPL) model of generalized fractional thermoelasticity theory with dual-phase-lags and two different fractional Orders, studied by Xu and Jiang [59], is obtained when $K^{*} = 0$ and $\alpha \neq \beta$.
- In this manuscript, we propose to study a new fractional thermoelasticity model characterized by three-phase-lags and three distinct fractional orders α, β and δ called here the generalized fractional thermoelasticity theory with three-phase-lags and denoted by (GFTPL).

Quintanilla and Racke [62] have analyzed the range of the parameters $\tau_{\mathbf{q}}$, τ_{θ}, τ_{ϑ}, K and K^{*} for the three-phase-lag theory to ensure the stability of the solutions of the heat conduction equation studied. In particular, he has shown that the condition $K^{*}\tau_{\vartheta} + K > K^{*}\tau_{\mathbf{q}}$ certifies the exponential stability of the solutions. The same author in [63] studied the well posedness of three-phase-lag models of heat conduction equation.

Following [71], the additional governing equations for a homogenous isotropic thermoelastic medium without external body forces are given below:

$$\sigma_{ij} = 2\mu e_{ij} + \lambda e_{kk}\delta_{ij} - \gamma\theta\delta_{ij} \tag{9}$$

$$2e_{ij} = u_{j,i} + u_{i,j} \tag{10}$$

$$\sigma_{ij,j} = \rho\frac{\partial^{2}u_{i}}{\partial t^{2}} \tag{11}$$

where σ_{ij} denotes the components of the stress tensor, e_{ij} denotes the components of the strain tensor and u_{i} denotes the component of the displacement vector.

FORMULATION OF THE PROBLEM

We consider the problem of a homogeneous, isotropic solid sphere of radius a. The medium is due to thermal shock and exposed to a time decaying heat source. We use the spherical coordinates (r, ξ, φ) where r is the radial coordinate, ξ is the co-latitude and φ the longitude of a spherical coordinate system.

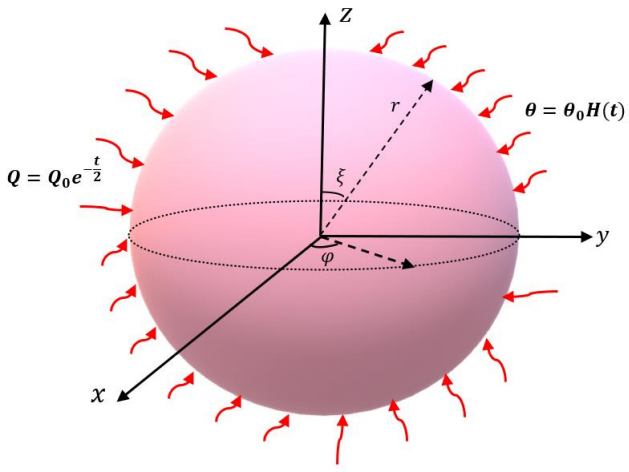

Fig. 1. Diagram of a thermoelastic rigid sphere due to thermal shock and heat generation

Due to spherical symmetry, one may express the state functions in terms of the radial distance r and time t. Thus, the displacement vector has the components

$$u_r = u(r,t),\ u_\xi(r,t) = u_\varphi(r,t) = 0 \tag{12}$$

The components of the strain tensor are

$$e_{rr} = \frac{\partial u}{\partial r}, \quad e_{\xi\xi} = e_{\varphi\varphi} = \frac{u}{r}, \quad e_{r\xi} = e_{r\varphi} = e_{\varphi\xi} = 0 \tag{13}$$

The cubic dilatation e is given by

$$e = \nabla.\mathbf{u} = \frac{1}{r^2}\ \frac{\partial(r^2 u)}{\partial r} = \frac{\partial u}{\partial r} + \frac{2u}{r} \tag{14}$$

The constitutive relations given in Eq. (9) can be derived

$$\begin{aligned} \sigma_{rr} &= 2\mu\ \frac{\partial u}{\partial r} + \lambda e - \gamma\theta \\ \sigma_{\xi\xi} &= 2\mu\ \frac{u}{r} + \lambda e - \gamma\theta = \sigma_{\varphi\varphi} \end{aligned} \tag{15}$$

In spherical coordinates, the equation of motion (12) turns into

$$\frac{\partial \sigma_{rr}}{\partial r} + 2\left(\frac{\sigma_{rr} - \sigma_{\varphi\varphi}}{r}\right) = \rho\frac{\partial^2 u}{\partial t^2} \tag{16}$$

From Eqs. (14), (15) and (16), yields

$$(\lambda + 2\mu)\frac{\partial e}{\partial r} - \gamma\frac{\partial \theta}{\partial r} = \rho\frac{\partial^2 u}{\partial t^2} \tag{17}$$

Applying the operator $1/r^2\ (\partial/\partial r)(r^2\ )$ to Eq. (17), we get

$$(\lambda + 2\mu)\nabla^2 e - \gamma\nabla^2\theta = \rho\frac{\partial^2 e}{\partial t^2} \tag{18}$$

where the Laplacien operator ∇^2 is given by

$$\nabla^2 = \frac{2}{r}\frac{\partial}{\partial r} + \frac{\partial^2}{\partial r^2} \tag{19}$$

Therefore, the heat equation appearing in Eq. (8) can be expressed as follows

$$\frac{\partial}{\partial t}\left(K + K^*\,\tau_\vartheta^\delta\ \frac{\partial^{\delta-1}}{\partial t^{\delta-1}}\right)\nabla^2\theta + \left(K^* + \ K\,\tau_\theta^\beta\ \frac{\partial^{\beta+1}}{\partial t^{\beta+1}}\right)\nabla^2\theta =$$

$$\left(1 + \tau_\mathbf{q}^\alpha\ \frac{\partial^\alpha}{\partial t^\alpha}\right)\left(\rho C_e\ \frac{\partial^2\theta}{\partial t^2} + \gamma T_0\ \frac{\partial^2 e}{\partial t^2} - \rho\ \frac{\partial Q}{\partial t}\right) \tag{20}$$

We will use the following non-dimensional parameters

$$\begin{aligned} \{r', u'\} &= c_1\eta\,\{r, u\}, \quad \left\{t', \tau_\mathbf{q}', \tau_\theta', \tau_\vartheta'\right\} = c_1^2\eta\left\{t, \tau_\mathbf{q}, \tau_\theta, \tau_\vartheta\right\}, \\ \theta' &= \frac{\gamma}{\rho c_1^2}\ \theta, \quad Q' = \frac{\gamma Q}{K c_1^4\eta^2}, \quad \sigma_{ij}' = \frac{\sigma_{ij}}{\rho c_1^2}, \quad \eta = \frac{\rho C_e}{K}, \ K^{*\prime} = \frac{K^*}{K c_1^2\eta}. \end{aligned} \tag{21}$$

where $c_1 = \sqrt{(\lambda + 2\mu)/\rho}$ is the dilatational wave velocity.

Using the non-dimensional parameters (21), we obtain (dropping the primes for convenience)

$$\frac{\partial}{\partial t}\left(1 + K^*\,\tau_\vartheta^\delta\ \frac{\partial^{\delta-1}}{\partial t^{\delta-1}}\right)\nabla^2\theta + \left(K^* + \tau_\theta^\beta\ \frac{\partial^{\beta+1}}{\partial t^{\beta+1}}\right)\nabla^2\theta = \left(1 + \tau_\mathbf{q}^\alpha\ \frac{\partial^\alpha}{\partial t^\alpha}\right)\left(\frac{\partial^2\theta}{\partial t^2} + \varepsilon_1\ \frac{\partial^2 e}{\partial t^2} - \frac{\partial Q}{\partial t}\right) \tag{22}$$

$$\nabla^2 e - \nabla^2\theta = \frac{\partial^2 e}{\partial t^2} \tag{23}$$

$$\begin{aligned} \sigma_{rr} &= b^2\ \frac{\partial u}{\partial r} + (1 - b^2)e - \theta \\ \sigma_{\xi\xi} &= b^2\ \frac{u}{r} + (1 - b^2)e - \theta = \sigma_{\varphi\varphi} \end{aligned} \tag{24}$$

where

$$b^2 = \frac{2\mu}{\lambda + 2\mu}, \quad \varepsilon = \frac{\gamma^2 T_0}{\rho^2 C_e c_1^2} \tag{25}$$

INITIAL AND BOUNDARY CONDITIONS

We take the initial conditions as follows

$$u(r,0) = \frac{\partial u(r,0)}{\partial t} = 0, \quad \theta(r,0) = \frac{\partial \theta(r,0)}{\partial t} = 0 \tag{26}$$

We suppose also that the following boundary conditions are hold:

(i) The surface of the sphere is due to thermal shock

$$\theta(a,t) = \theta_0 H(t), \ t > 0 \tag{27}$$

where $H(t)$ stands for the Heaviside function.

(ii) The surface of the sphere is traction free

$$\sigma_{rr}(a,t) = 0 \tag{28}$$

The temperature of the spherical medium is initially zero. For $t > 0$, the heat is generated or consumed within the medium at a time-dependent decaying generation rate, as in [72,73] described by the equation

$$Q(r,t) = Q_0 e^{-\frac{t}{2}} \tag{29}$$

in which Q_0 is the magnitude of the heat generation rate.

SOLUTION IN THE LAPLACE TRANSFORM DOMAIN

Applying the Laplace transformation technique, and relying on Lemma 2.24 of [68], our current problem changes into steady states. Therefore, Eqs. (22-24) turn, in the transform field, into

$$(\nabla^2 - a_1)\bar{\theta} = a_1 \varepsilon \bar{e} - a_1 \frac{\bar{Q}}{s} \tag{30}$$

$$(\nabla^2 - s^2)\bar{e} = \nabla^2 \bar{\theta} \tag{31}$$

$$\begin{aligned} \bar{\sigma}_{rr} &= b^2 \frac{\partial \bar{u}}{\partial r} + (1-b^2)\bar{e} - \bar{\theta} \\ \bar{\sigma}_{\xi\xi} &= b^2 \frac{\bar{u}}{r} + (1-b^2)\bar{e} - \bar{\theta} = \bar{\sigma}_{\varphi\varphi} \end{aligned} \tag{32}$$

where

$$a_1 = \frac{\left(1 + \tau_{\mathbf{q}}^{\alpha} s^{\alpha}\right) s^2}{s + K^* \tau_{\vartheta}^{\delta} s^{\delta} + K^* + \tau_{\theta}^{\beta} s^{\beta+1}} \quad and \ \bar{Q}(r,s) = \frac{2Q_0}{1+2\mathrm{s}}$$

Eliminating $\bar{\theta}$ from Eqs. (30) and (31), one gets

$$(\nabla^4 - A\nabla^2 + B)\bar{\theta} = C\bar{Q} \tag{33}$$

where the coefficients A, B and C are given by

$$A = \mathrm{s}^2 + a_1 + a_1\varepsilon, \ B = a_1 s^2, \ C = a_1 s \tag{34}$$

Since A and B are real positive numbers then Eq. (33) becomes

$$(\nabla^2 - m_1^2)(\nabla^2 - m_2^2)\ \bar{\theta} = C\bar{Q} \tag{35}$$

where m_1^2, m_2^2 are the roots of the characteristic equation

$$m^4 - Am^2 + B = 0 \tag{36}$$

The solution of Eq. (35) can be expressed by

$$\bar{\theta} = \frac{1}{\sqrt{r}} \sum_{i=1}^{2} A_i \, I_{\frac{1}{2}}(m_i r) + \frac{\bar{Q}}{s} = \sqrt{\frac{2}{\pi}} \sum_{i=1}^{2} \frac{A_i}{\sqrt{m_i}\, r} \sinh(m_i r) + \frac{\bar{Q}}{s} \tag{37}$$

where I_ν is the modified Bessel functions of the first kind of order $\nu \in \mathbb{R}$ and the parameters A_i, $(i = 1,2)$ can be calculated by the use of the boundary conditions. Similarly, the solution of $\bar{e}$ can be obtained as

$$\bar{e} = \sum_{i=1}^{2} \frac{A_i}{a_1 \varepsilon \sqrt{r}} (m_i^2 - a_1)\, I_{\frac{1}{2}}(m_i r) \tag{38}$$

From Eqs. (14) and (38), we find

$$\bar{u} = \sum_{i=1}^{2} \frac{A_i}{a_1 \varepsilon \sqrt{r}\, m_i} (m_i^2 - a_1)\, I_{\frac{3}{2}}(m_i r) \tag{39}$$

To obtain Eq. (39), we applied the following equality [74] of the Bessel functions

$$\int x^{\frac{3}{2}}\, I_{\frac{1}{2}}(x) dx = x^{\frac{3}{2}}\, I_{\frac{3}{2}}(x) \tag{40}$$

By differentiating Eq. (39) with respect to r, we get

$$\frac{\partial \bar{u}}{\partial r} = \sum_{i=1}^{2} \frac{A_i}{a_1 \varepsilon} (m_i^2 - q) \left(\frac{1}{\sqrt{r}}\, I_{\frac{1}{2}}(m_i r) - \frac{1}{r\sqrt{r}\, m_i}\, I_{\frac{3}{2}}(m_i r) \right) \tag{41}$$

In addition, the thermal stresses that appeared in Eq. (32) can be expressed as

$$\bar{\sigma}_{rr} = \sum_{i=1}^{2} A_i \left(\left(\frac{(m_i^2 - a_1)}{a_1 \varepsilon} - 1 \right) \frac{1}{\sqrt{r}}\, I_{\frac{1}{2}}(m_i r) - \left(\frac{b^2\,(m_i^2 - a_1)}{a_1 \varepsilon r \sqrt{r}\, m_i} \right) I_{\frac{3}{2}}(m_i r) \right) - \frac{\bar{Q}}{s} \tag{42}$$

$$\bar{\sigma}_{\xi\xi} = \sum_{i=1}^{2} A_i \left(\left(\frac{(1-b^2)(m_i^2 - a_1)}{a_1 \varepsilon \sqrt{r}} - 1 \right)\, I_{\frac{1}{2}}(m_i r) + \left(\frac{b^2 (m_i^2 - a_1)}{a_1 \varepsilon r \sqrt{r}\, m_i} \right) I_{\frac{3}{2}}(m_i r) \right) - \frac{\bar{Q}}{s} \tag{43}$$

Following [74], the expression of $I_\nu(x)$, for all positive number x, is given by

$$I_\nu(x) = \sum_{k=0}^{\infty} \frac{\left(\frac{x}{2}\right)^{\nu+2k}}{\Gamma(k+1)\, \Gamma(k+1+\nu)} \tag{44}$$

Setting $\nu = \frac{1}{2}$ and $\nu = -\frac{1}{2}$ in (44) and using the following formula for the gamma function

$$2^{2z-1} \Gamma(z)\, \Gamma\left(z + \frac{1}{2}\right) = \sqrt{\pi}\, \Gamma(2z), \quad Re(z) > 0 \tag{45}$$

we can deduce that

$$I_{\frac{1}{2}}(x) = \sqrt{\frac{2}{\pi}}\, \frac{\sinh(x)}{\sqrt{x}} \qquad \text{and} \qquad I_{-\frac{1}{2}}(x) = \sqrt{\frac{2}{\pi}}\, \frac{\cosh(x)}{\sqrt{x}} \tag{46}$$

Using the following recurrence relation

$$I_{\frac{3}{2}}(x) = I_{-\frac{1}{2}}(x) - \frac{1}{x}\, I_{\frac{1}{2}}(x) \tag{47}$$

we can write

$$I_{\frac{3}{2}}(x) = \sqrt{\frac{2}{\pi}}\, \frac{\left(\cosh(x) - \frac{\sinh(x)}{\sqrt{x}}\right)}{\sqrt{x}} \tag{48}$$

Performing Laplace transform, the expressions of the different physical variables can be written

$$\bar{\theta} = \sqrt{\frac{2}{\pi}}\, \sum_{i=1}^{2} \frac{A_i}{\sqrt{m_i}\, r}\, \sinh(m_i r) + \frac{\bar{Q}}{s} \tag{49}$$

$$\bar{e} = \sqrt{\frac{2}{\pi}}\, \sum_{i=1}^{2} \frac{A_i}{\sqrt{m_i}\, r\, a_1 \varepsilon}\, (m_i^2 - a_1) \sinh(m_i r) \tag{50}$$

$$\bar{u} = \sqrt{\frac{2}{\pi}}\, \sum_{i=1}^{2} \frac{A_i}{r a_1 \varepsilon} \frac{(m_i^2 - q)}{m_i^{\frac{3}{2}}} \left(\cosh(m_i r) - \frac{\sinh(m_i r)}{m_i r} \right) \tag{51}$$

$$\begin{aligned} \bar{\sigma}_{rr} = \sqrt{\frac{2}{\pi}}\, \sum_{i=1}^{2} A_i\, (m_i^2 - a_1) \Bigg(& \left(\frac{1}{a_1 \varepsilon} - 1 \right) \frac{1}{\sqrt{m_i}\, r} \sinh(m_i r) \\ & - \left(\frac{b^2}{a_1 \varepsilon r^2 m_i^{\frac{3}{2}}} \right) \left(\cosh(m_i r) - \frac{\sinh(m_i r)}{m_i r} \right) \Bigg) - \frac{\bar{Q}}{s} \end{aligned} \tag{52}$$

$$\bar{\sigma}_{\xi\xi} = \sqrt{\frac{2}{\pi}} \sum_{i=1}^{2} A_i (m_i^2 - a_1) \left(\left(\frac{(1-b^2)}{a_1 \varepsilon} - 1 \right) \frac{1}{\sqrt{m_i}\, r} \sinh(m_i r) + \left(\frac{b^2}{a_1 \varepsilon r^2 m_i^{\frac{3}{2}}} \right) \left(\cosh(m_i r) - \frac{\sinh(m_i r)}{m_i r} \right) \right) - \frac{\bar{Q}}{s} \tag{53}$$

Besides, the conditions (27) and (28), in the transform field, take the forms

$$\bar{\theta}(a, s) = \frac{\theta_0}{s}, \quad \bar{\sigma}_{rr}(a, s) = 0 \tag{54}$$

Substituting Eqs. (49) and (52) into the formulas of Eq. (54), we get two relations in the constants A_i, $i = 1,2$ as follows

$$\sqrt{\frac{2}{\pi}} \sum_{i=1}^{2} \frac{A_i}{\sqrt{m_i}\, a} \sinh(m_i a) = \frac{\theta_0}{s} - \frac{\bar{Q}}{s} \tag{55}$$

$$\sqrt{\frac{2}{\pi}} \sum_{i=1}^{2} A_i \, (m_i^2 - a_1) \left(\left(\frac{1}{a_1 \varepsilon} - 1 \right) \frac{1}{\sqrt{m_i}\, a} \sinh(m_i a) - \left(\frac{b^2}{a_1 \varepsilon a^2 m_i^{\frac{3}{2}}} \right) \left(\cosh(m_i a) - \frac{\sinh(m_i a)}{m_i a} \right) \right) = \frac{\bar{Q}}{s} \tag{56}$$

Solving this system, we obtain the values of the parameters A_i, $(i = 1,2)$. Thus, we get the expressions for the temperature, the displacement and the stress components of the medium in the Laplace transform domain.

Laplace transform inversion

So as to obtain the solutions of the different physical variables in the physical domain, it is unavoidable to apply the Laplace inversion to the obtained solutions in the transformed domain. In this paper, a precise and efficacious numerical method described by Dubner and Abate [75] and based on a Fourier series expansion is performed to obtain the inverse of the Laplace transform. An essential feature of this method is to be conceptually simple and easy to program. Specifically, authors have shown that any function f in Laplace domain takes the form $f(t) = f_c(t) - E(t)$ where f_c is the proposed approximation to f defined for $t \in [0, T]$ by:

$$f_c(t) = \frac{2e^{ct}}{T} \left(\frac{1}{2} Re \bar{f}(r, c) + Re \sum_{p=1}^{\infty} \bar{f} \left(r, c + \frac{ip\pi}{T} \right) \cos \left(\frac{p\pi}{T} t \right) \right) \tag{57}$$

Re is the real part, i is imaginary unit and c is any real positive number.

In the same article, the authors have shown that the error term E can become conveniently small by choosing suitably the parameter c and only for $t \leq \frac{T}{2}$. If one takes $t = \frac{T}{2}$ in (57), then f can be approximated to

$$f_c(t) = \frac{e^{ct}}{t} \left(\frac{1}{2} Re \bar{f}(r, c) + Re \sum_{n=1}^{N} \bar{f} \left(r, c + \frac{in\pi}{t} \right) (-1)^n \right) \tag{58}$$

where N is a finite number of terms.

Numerical results

We choose here the copper material to illustrate, by numerical evaluations, the analytic results obtained in the previous section. The constants of the problem given by [76-79] are

$\lambda = 7.76 \times 10^{10} (\text{kg m}^{-1}\text{s}^{-2})$, $\mu = 3.86 \times 10^{10} (\text{kg m}^{-1}\text{s}^{-2})$, $K = 386\ (\text{W m}^{-1}\text{K}^{-1})$, $C_E = 383.1 \times 10^3 (\text{J kg}^{-1}\ \text{K}^{-1})$, $\rho = 8954\ (\text{kg m}^{-3})$, $T_0 = 293(\text{K})$, $\alpha_t = 1.78 \times 10^5 (\text{K}^{-1})$

The computation was performed when $\theta_0 = 1$, $\tau_{\mathbf{q}} = 0.02$, $\tau_\theta = 0.03$, $\tau_\vartheta = 0.1$, which satisfies the condition $K^* \tau_\vartheta + K > K^* \tau_{\mathbf{q}}$, mentioned in section 2. The numerical method

described in the preceding section was applied to calculate temperature θ, radial displacement u, radial and hoop stresses σ_{rr} and $\sigma_{\varphi\varphi}$ inside the spherical solid $(a = 2)$.

The effects of different thermoelastic models with time-fractional derivatives $\alpha,\ \beta$ and δ and the effect of instant time t on the physical variables of the medium are analyzed. These distributions are illustrated in tables 1-4 and Figs. 2-13. The current results are well consistent with the theoretical solution.

The effect of time fractional derivatives $\alpha,\ \beta$ and δ

The effects of the fractional derivatives $\alpha,\ \beta$ and δ on the thermal reactions of the spherical solid are described in Tables 1-4 and Figures 2-5. It is gainful in this section to announce the results in tabular form to carry out the comparison between the different models of fractional thermoelasticity and to encourage other researchers to compare their numerical results and examine their precision.

In this case, we will study the effect of the thermoelastic models on the different physical fields in the direction of the radius r on the interval $0 \le r \le 2$. Numerical results are determined for the variations of temperature θ, displacement u and thermal stresses σ_{rr} and $\sigma_{\varphi\varphi}$ with various values of r. The valuation was carried out for the value $t = 0.1$ of the instant time and when the magnitude of the heat generation remains constant: $Q_0 = 0.1$. For the classical fractional models, the values of the fractional derivatives $\alpha,\ \beta$ and δ are taken as follows: FLS $(\alpha = 0.2)$, FDPL $(\alpha = \beta = 0.2)$, FTPL ($\alpha = \beta = \delta = 0.2$).

Through Tables 1-4, we will compare the results obtained in the new GFTPL model with the previous models (LS, DPL, GNIII, TPL, FLS, FDPL and FTPL). Figs. 2-5 represents the distribution of the different physical fields versus the radius r for five specific thermoelastic models (TPL, FLS, FDPL, FTPL and GFTPL). In Figs. 2-5, the new GFTPL models are represented by discontinuous curves: the case $\beta = \delta = 0.2,\ \alpha = 0.8$ is represented by the red curve, the case $\beta = \alpha = 0.2,\ \delta = 0.8$ by the green curve and the case $\alpha = \delta = 0.2,\ \beta = 0.8$ by the blue curve, while the other fractional models are represented by dashed curves and the black continuous curve represents the TPL model.

It is evident from the tables and the figures provided that the different variables are very sensitive to the parameters $\alpha,\ \beta$ and δ except for the displacement u where the effect is weak.

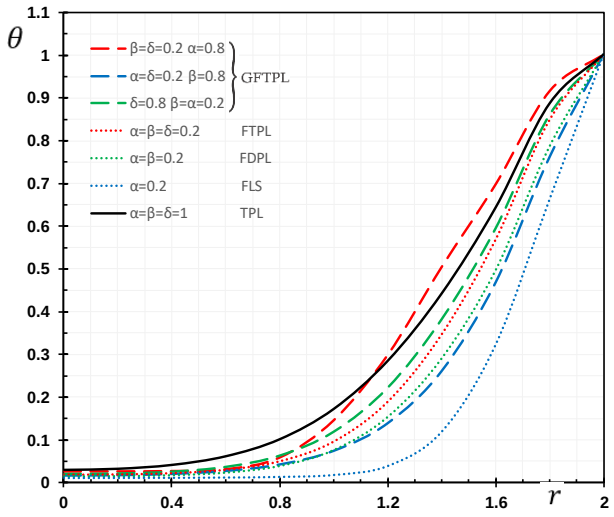

Fig. 2. Variation of the temperature θ versus radius r for different models of thermoelasticity

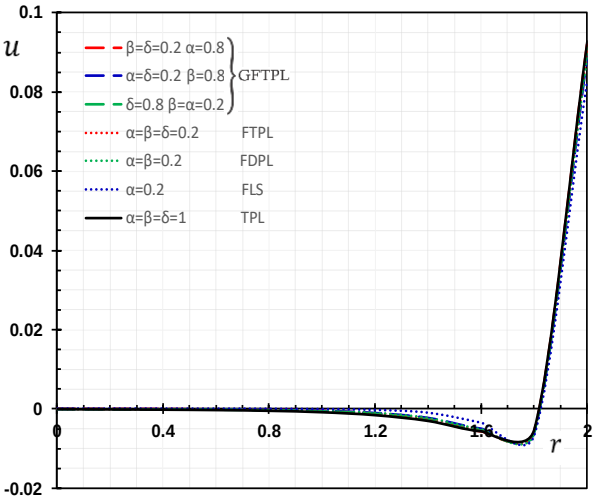

Fig. 3. Variation of the displacement u versus radius r for different models of thermoelasticity

Table 1. *Effect of different fractional thermoelastic models on the temperature θ*

r	LS	DPL	GNIII	TPL	FLS	FDPL	FTPL	GFTPL		
								α=β=0.**2** δ=0.**8**	α=δ=0.**2** β=0.**8**	δ=β=0.**2** α=0.**8**
0	0.0128195	0.0171868	0.0168506	0.0294872	0.0108644	0.0148205	0.018267	0.0203037	0.0165478	0.0256137
0.2	0.0128981	0.018277	0.0174544	0.032012	0.0109503	0.0153507	0.019008	0.0213749	0.0173884	0.025874
0.4	0.0136677	0.0223092	0.0198279	0.0410555	0.0112525	0.0174926	0.0219215	0.0256047	0.0204032	0.0266263
0.6	0.0151084	0.0319424	0.0263621	0.0613194	0.0119114	0.0235008	0.0298166	0.0367622	0.0273918	0.0308531
0.8	0.0173094	0.0527735	0.0434759	0.101201	0.0133229	0.0391663	0.0497956	0.0631791	0.0425374	0.058356
1	0.0201504	0.0945765	0.0847278	0.172108	0.0178609	0.0763733	0.0959596	0.119097	0.0744618	0.145464
1.2	0.0177457	0.171403	0.171501	0.284678	0.038811	0.153838	0.189076	0.222037	0.139069	0.298406
1.4	0.275791	0.299429	0.3242	0.442433	0.119122	0.290876	0.346822	0.38238	0.261197	0.504325
1.6	0.488705	0.497306	0.545757	0.643848	0.322908	0.497422	0.568847	0.595339	0.468699	0.697989
1.8	0.700777	0.782791	0.832844	0.887604	0.663564	0.787332	0.849173	0.860953	0.762377	0.916294
2	1.00234	1.00234	1.00234	1.00234	1.00234	1.00234	1.00234	1.00234	1.00234	1.00234

Table 2. *Effect of different fractional thermoelastic models on the displacement u*

r	LS	DPL	GNIII	TPL	FLS	FDPL	FTPL	GFTPL		
								α=β=0.**2** δ=0.**8**	α=δ=0.**2** β=0.**8**	δ=β=0.**2** α=0.**8**
0	-4.01987E-08	-1.15171E-07	-1.25632E-07	-2.31704E-07	-1.16718E-08	-9.72448E-08	-1.44349E-07	-1.69578E-07	-1.040E-07	-2.44E-07
0.2	-8.80543E-06	-0.000024494	-2.64706E-05	-4.84264E-05	-2.70351E-06	-2.06167E-05	-3.03015E-05	-3.54421E-05	-2.226E-05	-5.006E-05
0.4	-0.000024562	-5.88626E-05	-0.00006171	-0.000110895	-8.05494E-06	-4.89962E-05	-6.99669E-05	-8.10355E-05	-5.430E-05	-0.00010732
0.6	-5.66469E-05	-0.000119635	-0.000119055	-0.000210308	-2.11481E-05	-9.77336E-05	-0.000133376	-0.000153241	-0.00011174	-0.00018028
0.8	-0.000118245	-0.000242451	-0.000227315	-0.000393203	-5.34072E-05	-0.000195292	-0.000251646	-0.000288399	-0.00022666	-0.00029507
1	-0.000228309	-0.000509584	-0.000460833	-0.000756901	-0.000131977	-0.000415367	-0.000503407	-0.000574347	-0.00047194	-0.00056128
1.2	-0.000410431	-0.00110833	-0.0010119	-0.00149424	-0.000343536	-0.000947308	-0.00108485	-0.00121354	-0.00101859	-0.00125371
1.4	-0.00120974	-0.00244058	-0.00232745	-0.00295137	-0.0010573	-0.00223488	-0.00243362	-0.00262018	-0.00226223	-0.00282282
1.6	-0.00444626	-0.00519158	-0.00518098	-0.00556619	-0.00358902	-0.00508001	-0.00526877	-0.00540886	-0.00496473	-0.00574063
1.8	-0.00720259	-0.00576206	-0.00596856	-0.00508576	-0.00678974	-0.00605308	-0.00584562	-0.00561835	-0.00584106	-0.0055062
2	0.0865578	0.0898258	0.0898694	0.0926884	0.0830191	0.0891414	0.0904013	0.0912132	0.0887961	0.0926007

Table 1 and Fig. 2 represent the distribution of the thermodynamic temperature θ with respect to the distance r for the various thermoelastic models mentioned above. It is evident from Fig. 2 that the effect of the fractional derivatives α, β and δ on the thermodynamic temperature θ is significant. Inside the spherical solid, the solutions are different but the curves have a similar behavior except for the FLS model which clearly presents lower values than the other models. By comparing the FTPL model with the GFTPL new models, we notice that θ rises with the increase of the values of α and δ but decreases when β increases.

More precisely, the temperature θ starts at maximum value $\theta \approx 1$ on the surface of the solid sphere ($r = 2$), which fulfill the thermal boundary condition (27) of the problem and ensures that the numerical method used here is very reliable. Afterwards, the value gradually decreases by decreasing r to attain a minimum value close to zero around the center of the solid sphere. The temperature θ diminished much faster for the FLS model than that of all the other models, and the decrease of the TPL, FTPL and GFTPL (except the case $\alpha = \delta = 0.2, \beta = 0.8$) models is slower compared to other models. Table 1 reveals that the GFTPL model presents appropriate results for different values of the fractional-order α, β and δ.

Moreover, it is adequate to choose $\alpha = \beta = 0.2$ and $\delta = 0.8$ to acquire very close and accurate results.

Table 2 and Fig. 3 represent the variation of the radial displacement u through the radial direction of the spherical solid for the different thermoelastic models studied. It is evident from Table 2 and Fig. 3 that the fractional derivatives α, β and δ have a weak influence on the radial displacement u. Inside the solid sphere, the solutions are almost similar except the FLS model which presents slightly higher values than the other models. Moreover, we observe that the variation of u corresponding to different thermoelastic models follows a similar curve with a small change in values, restricted to a limited region $(1 \leq r \leq 2)$. Outside this interval, the variation will disappear identically. Fig. 3 shows that the displacement profile for the different models starts at a maximum value on the surface of the medium $(r = 2)$. After that, it diminishes rapidly with decreasing distance to attain a negative minimum value (near $r = 1.8$) and finally increases gradually until it reaches zero value around the center of the sphere.

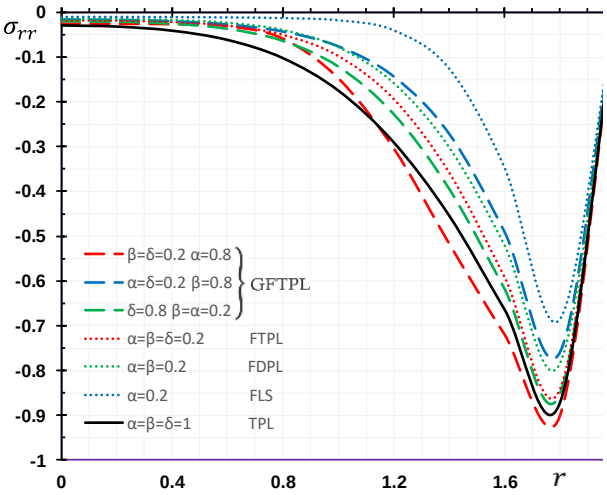

Fig. 4. Variation of the radial stress σ_{rr} versus radius r for different models of thermoelasticity

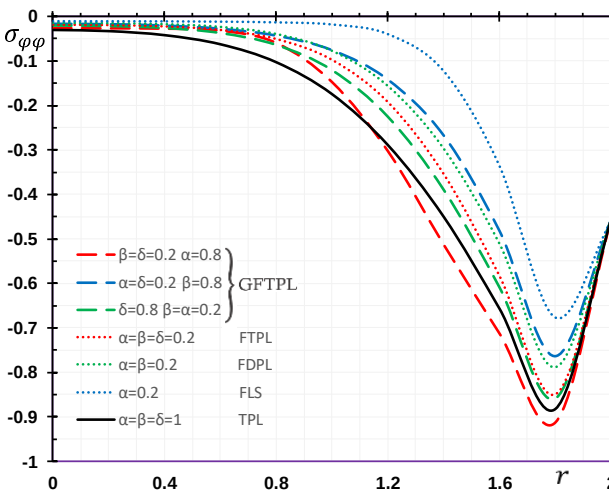

Fig. 5. Variation of the axial stress $\sigma_{\varphi\varphi}$ versus radius r for different models of thermoelasticity

Table 3. *Effect of different fractional thermoelastic models on the radial stress* $\boldsymbol{\sigma_{rr}}$

r	LS	DPL	GNIII	TPL	FLS	FDPL	FTPL	GFTPL α=β=0.2 δ=0.8	GFTPL α=δ=0.2 β=0.8	GFTPL δ=β=0.2 α=0.8
0	-0.0129	-0.0174174	-0.0171022	-0.0299512	-0.0108878	-0.0150152	-0.0185561	-0.0206433	-0.0167562	-0.0261024
0.2	-0.0129965	-0.0185373	-0.0177332	-0.0325184	-0.0109812	-0.0155691	-0.0193261	-0.0217455	-0.0176264	-0.026387
0.4	-0.0138386	-0.0226758	-0.0201992	-0.0417125	-0.0113128	-0.0177938	-0.0223385	-0.0260836	-0.0207456	-0.0272122
0.6	-0.0154235	-0.0325586	-0.0269396	-0.0623225	-0.0120465	-0.0239946	-0.0304555	-0.0374923	-0.0279715	-0.0315833
0.8	-0.0178761	-0.0539532	-0.0445211	-0.102948	-0.0136329	-0.0401121	-0.0509376	-0.0644861	-0.0436341	-0.0595271
1	-0.0211142	-0.09703	-0.0869134	-0.175405	-0.0185942	-0.0784357	-0.0983081	-0.121746	-0.0767077	-0.148118
1.2	-0.0191594	-0.176696	-0.176491	-0.291047	-0.0408633	-0.158656	-0.194306	-0.227707	-0.143925	-0.304664
1.4	-0.286054	-0.31079	-0.335618	-0.454469	-0.126316	-0.30208	-0.358428	-0.394285	-0.271956	-0.517355
1.6	-0.516384	-0.519752	-0.569117	-0.664323	-0.347361	-0.520908	-0.591846	-0.617607	-0.491241	-0.720292
1.8	-0.709294	-0.776203	-0.827382	-0.871619	-0.684261	-0.783907	-0.841801	-0.850449	-0.759046	-0.901174
2	2.112E-13	4.445E-12	-4.1051E-13	-3.5683E-12	-4.7969E-13	2.238E-12	7.876E-13	5.0101E-13	3.863E-12	3.474E-12

Table 4. *Effect of different fractional thermoelastic models on the hoop stress $\sigma_{\varphi\varphi}$*

r	LS	DPL	GNIII	TPL	FLS	FDPL	FTPL	GFTPL		
								α=β=0.**2** δ=0.**8**	α=δ=0.**2** β=0.**8**	δ=β=0.**2** α=0.**8**
0	-0.0129	-0.0174174	-0.0171022	-0.0299512	-0.0108878	-0.0150152	-0.0185561	-0.0206433	-0.0167562	-0.0261024
0.2	-0.0129914	-0.0185298	-0.0177263	-0.0325077	-0.0109793	-0.0155632	-0.0193188	-0.0217377	-0.0176189	-0.026381
0.4	-0.0138147	-0.0226399	-0.0201681	-0.0416617	-0.0113028	-0.0177659	-0.0223052	-0.0260471	-0.0207105	-0.027188
0.6	-0.0153607	-0.0324504	-0.0268497	-0.0621723	-0.0120143	-0.023911	-0.0303589	-0.0373833	-0.0278684	-0.0315192
0.8	-0.0177411	-0.0536676	-0.0442836	-0.102568	-0.013545	-0.0398842	-0.0506822	-0.0641943	-0.0433701	-0.0593115
1	-0.0208616	-0.0963154	-0.0862837	-0.174517	-0.0183603	-0.077822	-0.0976396	-0.120999	-0.076059	-0.147355
1.2	-0.018796	-0.174979	-0.174845	-0.289114	-0.0401258	-0.157041	-0.1926	-0.225889	-0.142351	-0.302587
1.4	-0.281799	-0.306865	-0.331584	-0.450572	-0.123482	-0.298087	-0.354376	-0.390217	-0.268204	-0.51287
1.6	-0.505355	-0.511799	-0.560701	-0.657586	-0.337406	-0.512366	-0.583665	-0.609878	-0.483098	-0.712753
1.8	-0.709042	-0.782686	-0.833418	-0.882413	-0.677706	-0.788973	-0.848721	-0.858805	-0.763948	-0.911769
2	-0.456652	-0.45502	-0.454998	-0.453591	-0.458419	-0.455362	-0.454733	-0.454327	-0.455534	-0.453634

Tables 3,4 and Fig. 4,5 depict the variation of thermal stresses σ_{rr} and $\sigma_{\varphi\varphi}$ versus the radius r of the spherical medium for the studied thermoelastic models. We notice that the fractional derivatives α, β and δ have a considerable impact on the profiles of thermal stresses. Inside the spherical solid, the solutions are different but the curves have a similar behavior except for the FLS model which clearly presents lower absolute values than the other models. By comparing the FTPL model with the GFTPL new models, we note that the absolute value of thermal stresses increase with the increase of the values of α and δ but decreases when β increases.

Also, Fig. 4,5 show that the results given by the GFTPL models are physically acceptable and accurate especially when $\alpha = \beta = 0.2$ and $\delta = 0.8$. The variation of thermal stresses σ_{rr} and $\sigma_{\varphi\varphi}$ for the FLS model decays slower than all the other models and reaches more rapidly a steady-state lower and close to zero.

Moreover, we observe that the variation of thermal stresses corresponding to different thermoelastic models follows a similar curve with a small change in values, restricted to a limited region ($0.6 \leq r \leq 1.8$). Outside this region, the variation will disappear gradually.

It is obvious from Fig. 4 that the graph of σ_{rr} for different models starts with a zero value at the surface of the medium, achieving the boundary condition (28), then, it decreases rapidly with decreasing r to attain a negative minimum value (near $r = 1.8$) and finally increases gradually with decreasing r until it reaches the steady-state.

We note from Fig. 5 that the profile of $\sigma_{\varphi\varphi}$ starts with a common negative value $\sigma_{\varphi\varphi} \approx -0.45$ and then follows an identical behavior to the profile of σ_{rr}.

We remark that the profiles of the thermodynamic temperature θ and the radial thermal stress σ_{rr} described in this paragraph harmonize with the results of Youssef [56] and Abouelregal [61].

The effect of different thermoelastic models versus the instant time

This section describe the effect of different thermoelastic models on the non-dimensional temperature, displacement and thermal stresses at different values of the instant time t in the range $0 \leq t \leq 0.45s$ at a fixed radius ($r = 1.6$) and when the magnitude Q_0 remains constant ($Q_0 = 0.1$). The values of different fields are plotted in Figs. 6-9. The influence of the instant time parameter t is much apparent in all physical fields.

The boundary condition (26) is attained since the value of the temperature θ (displacement u) is 0 at the beginning of the process ($t = 0$). This last result is clear from Fig. 6 (Fig. 7) despite that the method used here does not allow us to obtain the exact value of any physical fields at $t = 0$.

We notice in Fig. 6 (and other results that we omitted here for the convenience of the reader) that after a certain time, the temperature attains its steady state. This is consistent with real experiments and matches with the results of Youssef [56] and Xu [58, 59]. Besides, the behaviour of the curve of the different physical fields in our model is very semblable to those obtained in these published articles.

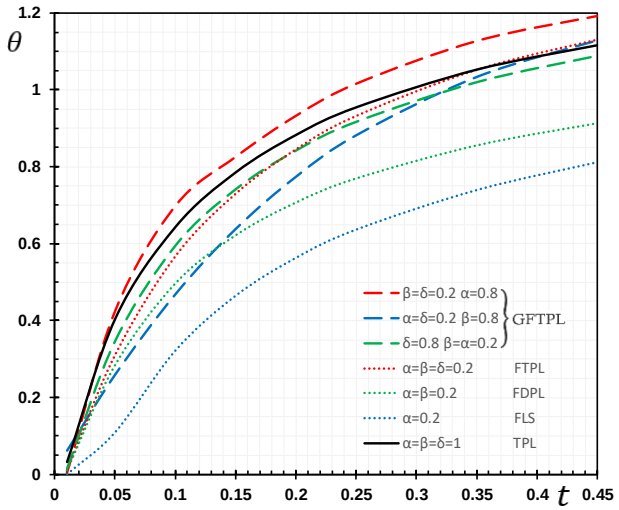

Fig. 6. Variation of the temperature θ versus instance t or different models of thermoelasticity

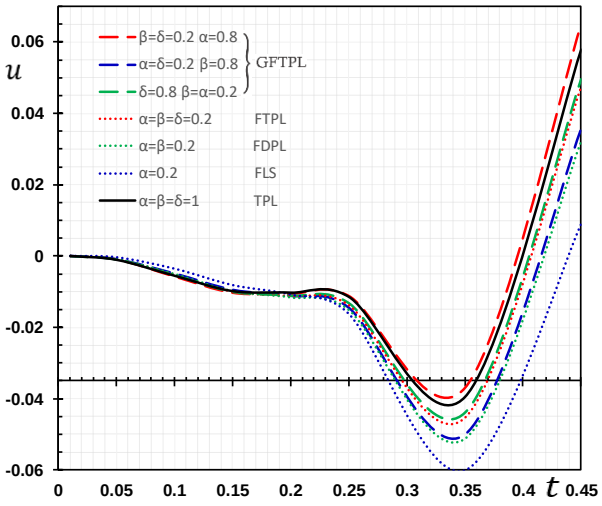

Fig. 7. Variation of the displacement u versus instance t for different models of thermoelasticity

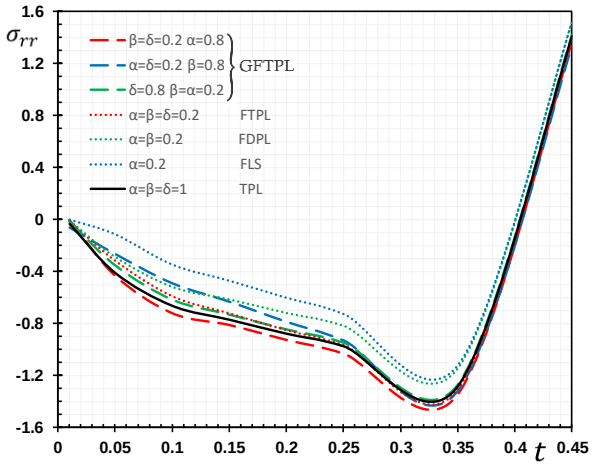

Fig. 8. Variation of the radial stress σ_{rr} versus instance t for different models of thermoelasticity

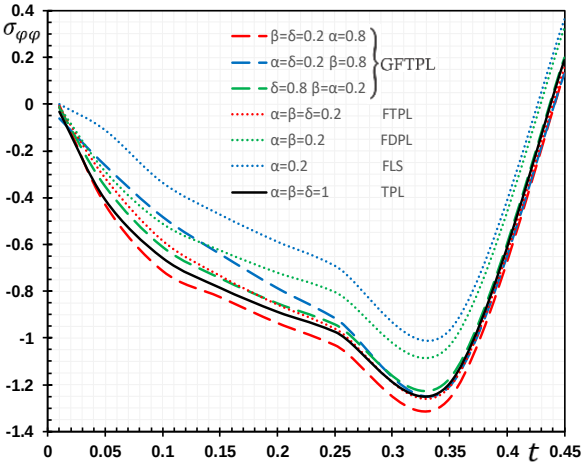

Fig. 9. Variation of the axial stress $\sigma_{\varphi\varphi}$ versus instance t for different models of thermoelasticity

Simultaneous effect of the instant time and radius

This last section illustrates how the non-dimensional temperature, displacement and thermal stresses differ with different values of the instant time t ($0.1s \leq t \leq 0.2s$) all over the spherical medium ($0 \leq r \leq 2$) in the situation of the GFTPL model $\alpha = \delta = 0.2$ and $\beta = 0.8$ and when the magnitude Q_0 remains constant ($Q_0 = 0.1$). The values of different fields are plotted in Figs. 10-13. The influence of the instant time parameter t is much manifest in all physical fields distributions. We note that all studied fields attain their boundary values conditions recommended in the model.

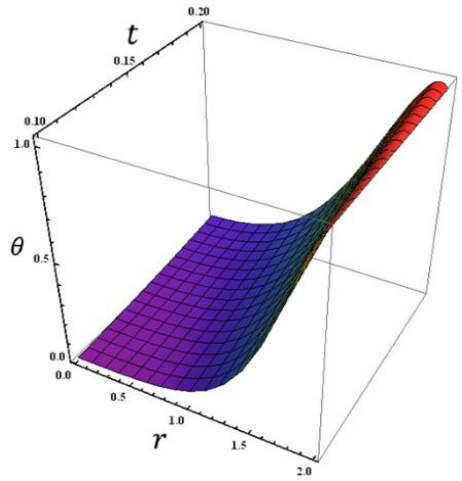

Fig. 10. Variation of the temperature θ versus radius r and time t

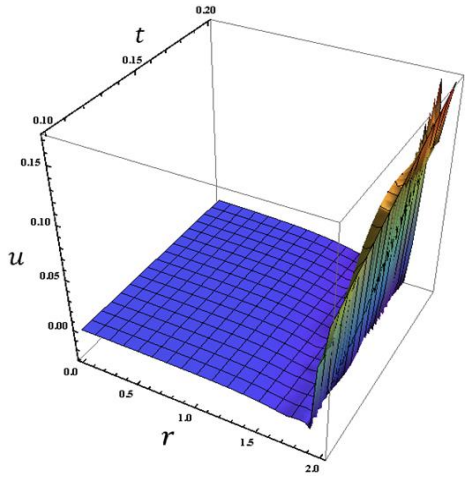

Fig. 11. Variation of the displacement u versus radius r and time t

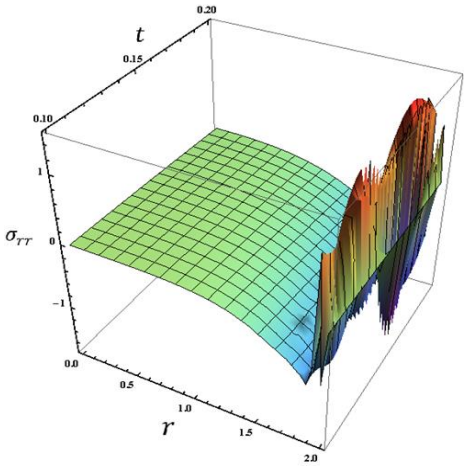

Fig. 12. Variation of the radial stress σ_{rr} versus radius r and time t

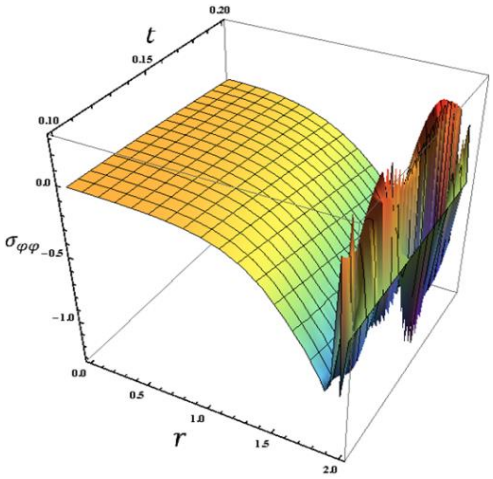

Fig. 13. Variation of the hoop stress $\sigma_{\varphi\varphi}$ versus radius r and time t

Fig. 10 shows that the temperature θ increases inside the medium with the increase of the parameter t to reach a maximum value at the instant $t \approx 0.2s$. However, the parameter t presents a weak influence on the temperature θ on the surface of the spherical medium and the value of θ is equal to 1 which agrees with the boundary condition (27).

We observe from Fig. 11 that the parameter t presents a weak influence on the displacement u in the range $0 < r < 0.8$ and the value of u is almost equal to 0 in this range. Then, the displacement u decreases slightly with the increase of t in the range $0.8 < r < 1.8$ and finally increases around the surface of the medium.

It is evident from Figs. 12 and 13 that the thermal stresses σ_{rr} and $\sigma_{\varphi\varphi}$ decrease inside the medium with the increase of the instant time t in the range $0 < r < 1.7$. Figs. 12 and 13 show that over time the temperature changes, causing stresses on the stressed surface as a result of thermal shock, which may lead to crack formation and propagation. It is also clear from the figures the prominent effect of time on the areas of thermal stresses. The instant time parameter t presents a weak effect on the thermal stresses on the surface of the medium.

Indeed, the value of $\sigma_{\varphi\varphi}$ is almost equal to -0.45 on the surface of the solid sphere and the value of σ_{rr} is equal to 0 which is compatible with the mechanical boundary condition (28). Thermal stress may have detrimental effects on the performance of some thermoelastic devices if thermomechanical processes are unable to control rapid increases in core temperature. For an improved design, it is critical to investigate the highest possible heat dissipation capacity and the highest possible produced thermal stresses. Since there is a steady influx of new materials and functional features thanks to progress in material processes, it is necessary to unearth the materials' latent mechanical potential.

CONCLUSIONS

In this work, a thermoelastic model with three different fractional-order-derivatives and three phase-lags for a homogeneous isotropic solid sphere has been investigated. The medium is subjected to thermal shock as well as a decaying generation rate. All the associated equations have been completely solved using the Laplace transform technique and an accurate numerical inversion method. A comparison is made to show the dependence of all field variables on fractional-order parameters α, β and δ associated with the different models of thermoelasticity studied. The effect of the instant time is also discussed. From the numerical results, most fields are very responsive to the variation of the fractional derivatives α, β, δ and the instant time. The results are physically acceptable and accurate for the different models of thermoelasticity and especially when $\alpha = \beta = 0.2$ and $\delta = 0.8$.

The validity of results is acceptable by comparing the temperature, displacement, and thermal stresses according to the new GFTPL model with those due to other thermoelasticity models.

The results presented in this article are useful for studying thermoelastic deformations in solid mechanics. Furthermore, fractional thermoelastic models are all-important for the development of new materials.

Declarations:

Data Availability
All data were included in the manuscript.
Conflict of Interest
The authors declared no potential conflicts of interest with respect to the research, authorship and publication of this article.
Funding
The authors received no financial support for the research, authorship and publication of this article.
ORCID iD
Anouar Saidi https://orcid.org/0000-0002-1147-5488

REFERENCES

1. Neumann F.E.: Vorlesungen über die theorie der elasticität der festen körper und des lichtäthers, Leipzig B.G. Teubner, 1885.
2. Duhamel J.H.: Second mémoire sur les phénomènes thermo-mécaniques. Journal de L'Ecole Polytechnique 15(25) (1837) 1-57.

3. Biot M.A.: Thermoelasticity and irreversible thermodynamics. Journal of Applied Physics 27(3) (1956) 240–253.
4. Cattaneo C.: Sur une forme de l'équation de la chaleur éliminant le paradoxe d'une propagation instantanée. Comptes Rendus de l'Académie des Sciences 247 (1958) 431–433.
5. Cattaneo C.: Sulla Condizione Del Calore. Atti del Seminario Matematico e Fisico dell'Università di Modena e Reggio Emilia 3 (1948) 83-101.
6. Vernotte P.: Les paradoxes de la théorie continue de l'équation de la chaleur. Comptes Rendus de l'Académie des Sciences 246 (1958) 3154–3155.
7. Lord H.W. and Shulman Y.: A generalized dynamic theory of thermoelasticity. Journal of the Mechanics and Physics of Solids 15(5) (1967) 299–309.
8. Green A.E. and Lindsay K.A.: Thermoelasticity. Journal of Elasticity 2(1) (1972) 1–7.
9. Tzou D.Y.: A unified approach for heat conduction from macro-to micro-scales. Journal of Heat Transfer 117(1) (1995) 8–16.
10. Tzou D.Y.: The generalized lagging response in small-scale and high-rate heating. International Journal of Heat and Mass Transfer 38(17) (1995) 3231–3240.
11. Tzou D.Y.: Experimental support for the lagging behavior in heat propagation. Journal of Thermophysics and Heat Transfer 9(4) (1995) 686–693.
12. Antaki P.: Solution for non-Fourier dual phase lag heat conduction in a semi-infinite slab with surface heat flux. International Journal of Heat and Mass Transfer 41(14) (1998) 2253-2258.
13. Jiang F.M., Liu D.Y. and Zhou J.H.: Non-Fourier heat conduction phenomena in porous material heated by microsecond laser pulse. Nanoscale and Microscale Thermophysical Engineering 6(4) (2003) 331-346.
14. Zhou J. H., Chen J. K., and Zhang Y.W.: Dual-phase lag effects on thermal damage to biological tissues caused by laser irradiation. Computers in Biology & Medicine 39(3) (2009) 286-293.
15. Zhang Y. W.: Generalized dual-phase lag bioheat equations based on nonequilibrium heat transfer in living biological tissues. International Journal of Heat and Mass Transfer 52(21-22) 2009 4829-4834,.
16. Lee H.L., Chen W.L., Chang W.J., Wei E.J. and Yang Y.C.: Analysis of dual-phase-lag heat conduction in short-pulse laser heating of metals with a hybrid method. Applied Thermal Engineering 52(2) 2013 275-283.
17. Green A.E. and Naghdi P.M.: A Re-Examination of the basic postulates of thermomechanics Proceedings: Mathematical and Physical Sciences 432(1885) (1991) 171–194.
18. Green A.E. and Naghdi P.M.: On undamped heat waves in an elastic solid. Journal of Thermal Stresses 15(2) (1992) 253–264.
19. Green A.E. and Naghdi P.M.: Thermoelasticity without energy dissipation. Journal of Elasticity 31(3) (1993) 189–208.
20. Roychoudhuri S.: On a thermoelastic three-phase-lag model. Journal of Thermal Stresses 30(3) (2007) 231–238.
21. Sprague G. H. and Huang P. C.: Behavior of Aircraft Structures under Thermal Stress. SAE Transactions 66 (1958) 457–465.
22. Buettner K.J.K.: Thermal stresses in the modern aircraft. Archiv für Meteorologie, Geophysik und Bioklimatologie, Serie B 5 (1954) 377–387.

23. Loveless E. and Boswell A.C.: The Problem of Thermal Stresses in Aircraft Structures: A Paper Presented at the Bristol Conference on Thermal Stress Organized by the Stress Analysis Group of the Institute of Physics on January 7, 1954, Aircraft Engineering and Aerospace Technology 26(4) (1954) 122-124.
24. Rolfes R. Teßmer J. and Rohwer K.: Models and Tools for Heat Transfer, Thermal Stresses and Stability of Composite Aerospace Structures. Journal of Thermal Stresses 26 (2003) 641-670.
25. Capey E.C.: Alleviation of thermal stresses in aircraft structures. Aeronautical Research Council Current Papers Ministry of Aviation; Royal Aircraft Establishment; RAE Farnborough (1965)
26. Baczynski Z.F. and Ignaczak: Thermoelastic stress analysis of reactor secondary containment. J. Boley, B.A. [ed.], Netherlands: North-Holland 1977.
27. Alujevic A., Cernej B., Potrc I. and Skerget L.: Boundary element method for thermoelasticity of nuclear reactors. ETAN '81: 25 Conference of the Society for Electronics, Telecommunications, Computers, Automation, and Nuclear Engineering, Yugoslavia: Society for Electronics, Telecommunications, Automation, and Nuclear Engineering (1981).
28. Yuan B., Zheng J., Wang J., Zeng H., Yang W., Huang H. and Zhang S. Numerical Calculation Scheme of Neutronics-Thermal Mechanical Coupling in Solid State Reactor Core Based on Galerkin Finite Element Method. Energies 16 (2023) 659.
29. Hoffman R.E. and Ariman, T.: Thermal and mechanical stresses in nuclear reactor vessels. Nuclear Engineering and Design 20(1) (1972) 31-55.
30. Leccese G., Bianchi D., Betti B., Lentini D. and Nasuti F.: Convective and Radiative Wall Heat Transfer in Liquid Rocket Thrust Chambers. Journal of Propulsion and Power 34(2) (2018) 318–326.
31. Chryssolouris G.: Laser machining, theory and practice. Springer, New York, 1991.
32. Dominiczak K., Rzadkowski R. and Radulski W.: Thermoelastic Steam Turbine Rotor Control Based on Neural Network. In: Pennacchi, P. (ed.) Proceedings of the 9th IFToMM International Conference on Rotor Dynamics. Mechanisms and Machine Science, 21. Springer, Cham (2015).
33. Dominiczak K. and Banaszkiewicz M.: A verification approach to thermoelastic steam turbine rotor analysis during transient operation. Transactions IFFM 131 (2016) 55–65.
34. Banaszkiewicz M. and Badur J.: Practical Methods for Online Calculation of Thermoelastic Stresses in Steam Turbine Components. Selected Problems of Contemporary Thermomechanics. InTech. (2018).
35. Pertz G. H. and Gerhardt C. J.: Leibnizens gesammelte Werke, Lebinizens mathematische Schriften, Erste Abtheilung, Band II, 301-302. Dritte Folge Mathematik (Erster Band). A. Asher & Comp., Briefwechsel zwischen Leibniz, Hugens van Zulichem und dem Marquis de l'Hospital, 1849.
36. Lacroix S.F.: Traité du calcul différentiel et du calcul intégral Tome 2. Paris: Courcier, 1814.
37. Liouville J.: Mémoire sur le calcul des différentielles à indices quelconques. Journal de l'École polytechnique 13 (21. cah.) (1832) 71–162.
38. Liouville J.: Memoire sur l'integration des equations différentielles à indices fractionnaires. Journal de l'École polytechnique 15(55) (1837) 58-84.
39. Fourier J.: Théorie analytique de la chaleur, Paris, 1822.
40. Riemann B.: Versuch einer allgemeinen Auffassung der Integration und Differentiation. Gesammelte Mathematische Werke und Wissenschaftlicher Nachlass. Teubner, Leipzig 1876

(Dover, New York, 1953) 331-344.

41. Sonin N.Y.: On differentiation with arbitrary index. Moscow, Matematicheskii Sbornik 6(1) (1869) 1-38.
42. Laurent H.: Sur le calcul des dérivées à indices quelconques. Nouvelles Annales de Mathématiques 3(3) (1884) 240-252.
43. Grunwald A. K.: Uber "begrenzte" Derivationen und deren Anwendung. Zeitschrift für angewandte Mathematik und Physik 12 (1867) 441-480.
44. Weyl H.: Bemerkungen zum Begriff des Differentialquotienten gebrochener Ordnung. Vierteljahresschrift der Naturforsch. Ges. Zürich, 62 (1917) 296.
45. Lazarevi M.: Advanced topics on applications of fractional calculus on control problems. System Stability and Modeling, WSEAS Press, Belgrade, Serbia, 2012.
46. Machado J. A. T.: Fractional Calculus: Application in control and robotics. Advances in Mobile Robotics (2008).
47. Ferreira N., Duarte F., Lima M., Marcos M. and Machado J.A.T.: Application of fractional calculus in the dynamical analysis and control of mechanical manipulators. Fractional Calculus and Applied Analysis 11(1) (2008) 91-113.
48. Henry B. and Wearne S.: Existence of Turing instabilities in a two-species fractional reaction–diffusion system. SIAM Journal on Applied Mathematics 62 (2002) 870–887.
49. Metzler, R. and Klafter J.: The random walk's guide to anomalous diffusion: a fractional dynamics approach. Physics Reports 339 (2000) 1-77.
50. Engheia N.: On the role of fractional calculus in electromagnetic theory. IEEE Antennas and Propagation Magazine 39 (1997) 35-46.
51. Ionescu C., Lopes A., Copot D., Machado J. A. T. and Bates J. H. T.: The role of fractional calculus in modeling biological phenomena: A review. Communications in Nonlinear Science and Numerical Simulation 51 (2017) 141–159.
52. Schiesse H., Metzlert R., Blument A. and Nonnemacher T.F.: Generalized viscoelastic models: their fractional equations with solutions. Journal of Physics A: Mathematical and General 28 (1995) 6567-6584.
53. Heymans N. and Bauwens J.-C.: Fractal rheological models and fractional differential equations for viscoelastic behavior. Rheologica Acta 33 (1994) 210–219.
54. Povstenko Y.Z.: Fractional heat conduction equation and associated thermal Stresses. Journal of Thermal Stresses 28 (2005) 83–102.
55. Povstenko Y.Z.: Fractional radial heat conduction in an infinite medium with a cylindrical cavity and associated thermal stresses. Mechanics Research Communications 37 (2010) 436–440.
56. Youssef H. M.: Theory of Fractional Order Generalized Thermoelasticity. Journal of Heat Transfer 132(6) (2010) 061301.
57. Sherief H.H., El-Sayed A.M.A. and Abd El-Latief A.M.: Fractional order theory of thermoelasticity. International Journal of Solids and Structures 47 (2010) 269–275.
58. Xu H., Wang X. and Qi H.: Fractional dual-phase-lag heat conduction model for laser pulse heating, 29th Chinese Control And Decision Conference (CCDC), (2017).
59. Xu H. and Jiang X.: Time fractional dual-phase-lag heat conduction equation. Chinese Physics B 24 (3) (2015).
60. Ezzat M. A., El Karamany A. S. and Fayik M. A.: Fractional order theory in thermoelastic

solid with three-phase lag heat transfer. Archive of Applied Mechanics 82(4) (2012) 557- 572.

61. Abouelregal A. E.: Three-phase-lag thermoelastic heat conduction model with higher-order time-fractional derivatives. Indian Journal of Physics 94 (2020)1949–1963.
62. Quintanilla R. and Racke R.: A note on stability in three-phase-lag heat conduction. International Journal of Heat and Mass Transfer 51 (2008) 24–29.
63. Quintanilla R.: A well-posed problem for the three-dual-phase-lag heat conduction, Journal of Thermal Stresses 32(12) (2009) 1270–1278.
64. Chiriţă S., D'Apice C. and Zampoli V.: The time differential three-phase-lag heat conduction model: thermodynamic compatibility and continuous dependence. International Journal of Heat and Mass Transfer 102 (2016) 226-232.
65. Xu M. and Tan W.: Intermediate processes and critical phenomena: Theory, method and progress of fractional operators and their applications to modern mechanics. Science In China Series G-Physics Astronomy 49 (2006) 257–272.
66. Klafter J., Sokolov I.M.: Anomalous diffusion spreads its wings. Physics World 18 (2008) 29–32.
67. Li H.B. and Li Z.: Anomalous energy diffusion and heat conduction in one-dimensional system. Chinese Physics B 19(5) 2010.
68. Kilbas A.A., Srivastava H. M. and Trujillo J.J.: Theory and Applications of Fractional Differential Equations. North-Holland Mathematics Studies 204 (2006) 69-133.
69. Machado J.T., Kiryakova V. and Mainardi F.: Recent history of fractional calculus. Communications in Nonlinear Science and Numerical Simulation 16 (2011) 1140–1153.
70. Podlubny I.: Fractional Differential Equations, Academic Press, New York, 1999.
71. Hetnarski R.B. and Eslami M.R.: Basic Laws of Thermoelasticity. In: Thermal Stresses – Advanced Theory and Applications. Solid Mechanics and its Applications, 158. Springer, Dordrecht, 2019, pp.1-43.
72. Giraud A. and Rousset, G. Thermoelastic and thermoplastic response of a porous space submitted to a decaying heat source. International Journal for Numerical and Analytical Methods in Geomechanics 19(7) (1995) 475–495.
73. Claesson, J. and Probert, T.: Thermoelastic stress due to a rectangular heat source in a semi-infinite medium. Presentation of an analytical solution. Engineering Geology 49(3-4) (1998) 223–229.
74. Lebedev N. N.: Special functions and their applications. Translated from the Russian by R. A. Silverman. Englewood Cliffs, N.J.: Prentice Hall, Inc. (1965).
75. Dubner H. and Abate J.: Numerical inversion of Laplace transforms by relating them to the finite Fourier cosine transform. Journal of the ACM, 15(1) (1968) 115–123.
76. Sokolnikoff I.S.: Mathematical Theory of Elasticity, New York, Dover, 1946.
77. Thomas L.C: Fundamentals of Heat Transfer, Prentice-Hall Inc., Englewood Cliffs, New Jersey, 1980.
78. Abouelregal A. E.: Fractional heat conduction equation for an infinitely generalized thermoelastic long solid cylinder. International Journal for Computational Methods in Engineering Science and Mechanics 17(5-6) 2016 374–381.
79. Aouadi M.: A problem for an infinite elastic body with a spherical cavity in the theory of generalized thermoelastic diffusion. International Journal of Solids and Structures 44(17) (2007) 5711–5722